Characterization of Shallow Water Environments and Waveform Design for Diversity

Ye Jiang, Hao Shen and Antonia Papandreou-Suppappola

Department of Electrical Engineering
Fulton School of Engineering, Arizona State University, Tempe, AZ
jiangye@asu.edu, hao_shen@asu.edu and papandreou@asu.edu

Keywords: Time-varying system, dispersive environment, waveform diversity, shallow water acoustics.

ABSTRACT

In this paper, we investigate the dispersive characterization of shallow water environments for acoustic transmissions, and we develop a time-varying system representation to model its dispersive propagation characteristics. We also obtain the discrete model of this representation using a transform-based approach or by nonlinearly warping the discrete time-frequency model of narrowband environments. Using this discrete model in a shallow water communication application, we design a wideband time-varying waveform to match the dispersive nature of the environment. As we demonstrate with numerical results, the design can provide dispersive Doppler diversity by employing maximal ratio combining techniques.

1. INTRODUCTION AND MOTIVATION

Time-varying system representations based on spreading functions are important in many applications as they can provide a physical interpretation of the effects of the system on the input signal [1]. However, spreading function representations are not practical as they are based on continuous formulations of the signal transformations with an uncountably infinite set of parameters. Discrete equivalent representations can be derived with a countably infinite or (under certain physical assumptions on the system) a finite number of sampled parameters [2, 3]. More importantly, the modular structure of such discrete formulations can be exploited for system analysis as well as provide receiver performance improvements. For example, the tapped-delay line model based on a weighted summation of discrete time shifts can lead to multipath diversity from a frequency-selective channel [4].

In shallow water environments, acoustic transmission is subjected to multipath propagation [1] as well as frequency-dependent group velocity dispersion [5]. The multipath is due to boundary reflections whereas the dispersion is the result of shallow waveguide propagation. These effects can severely limit the performance of underwater acoustic applications such as sonar and communications [6, 7]. In communication systems, transmitted waveform design and diversity processing schemes can effectively combat these degradations and improve bit error rate performance. However, such schemes require accurate and effective models to characterize the propagation environment. For shallow water acoustic transmission, although the structure of the arrival signal has been well-studied in terms of multipath and mode dispersion [5, 6, 7, 8], the time-varying environment has not been represented in a characteristic model.

In this paper, we propose a time-varying system representation to model the dispersive propagation characteristics of the shallow water environment. This representation is in terms of a dispersive spreading function that characterizes the effect of multipath and dispersion on the propagation waveform. We employ two different approaches to develop a discrete representation model for the dispersive shallow water environment. The first approach uses the Fourier transform to uniformly sample the time shift and dispersive frequency shift parameters. The second approach warps a unitarily equivalent model for narrowband systems. Based on this proposed discrete environment model, we design an appropriate waveform to exploit some potential diversity and thus increase receiver processing performance. Specifically, we develop a time-varying waveform to match the dispersion property of the shallow water environment and to achieve dispersive Doppler diversity using maximal ratio combining (MRC) techniques [4] for underwater communications. We demonstrate that our proposed discrete dispersive modeling and processing can exploit this inherent diversity and yield higher performance than narrowband schemes.

The paper is organized as follows. We present the shallow water environment characteristics in Section 2. In Section 3, we present the system model and its discretization based on the dispersive spreading function. In Section 4, we investigate the application of the proposed model in shallow water communications, and we design the transmitted waveform to exploit dispersive diversity. In Section 5, we demonstrate the advantage of our proposed waveform in shallow water communications with theoretical analysis and numerical results.

2. SHALLOW WATER ENVIRONMENT CHARACTERISTICS

Shallow acoustic transmission is adversely affected by both multipath propagation and frequency-dependent group velocity dispersion. Intensive boundary interactions make sound propagation analogous to electromagnetic propagation in dielectric waveguides [5, 7]. Specifically, at depth d, waveguide theory using normal modes shows that the group velocity at the mth mode for frequency f is given by $U_m(f) = c\sqrt{1-\frac{f_m^2}{f^2}}$, where c is the speed of sound in water, and $f_m = m\,c/(2\,d)$ is the cutoff frequency of the mth mode.

Due to the varying group velocity, if the transmitter and receiver are separated by a radial distance R, then the transmitted signal $x(t)$ will asymptotically arrive at the mth mode phase-modulated by the nonlinear time-varying phase

$$\phi(t) = 2\pi f_m(t^2-\alpha^2)^{\frac{1}{2}} \qquad (1)$$

where $\alpha = R/c$. The phase in (1) was obtained using the method of stationary phase assuming $t \gg \alpha$ [5]. We plotted the characteristic dispersive instantaneous frequency $\frac{d}{dt}\phi(t) = f_m t/(t^2-\alpha^2)^{1/2}$ in Figure 1, for the first 6 modes with $c = 1500$ m/s, $d = 100$ m and $R = 30$ km. In [8], these numerically generated curves were compared to time-frequency representations of received acoustic signals from explosive sources in an ocean bottom interaction experiment. As the theoretical and experimental results were found in agreement in [8], the use of the nonlinear phase function in (1) is justified for describing the dispersion behavior of the shallow water acoustic modes.

3. DISPERSIVE CHARACTERIZATION OF SHALLOW WATER ENVIRONMENTS

3.1. Dispersive Spreading Function Representation

In order to develop a characterization for the dispersive environment, we consider a specific multipath arrival through the shallow water associated with propagation distance d resulting in time delay $\tau = d/c$. The received signal $y(t)$ at

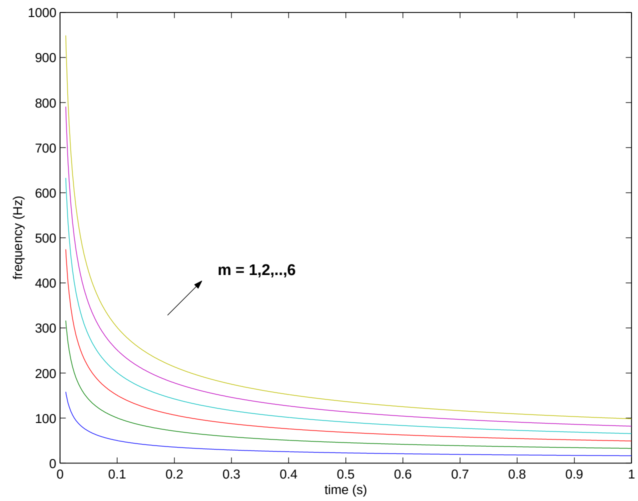

Fig. 1. Time-frequency dispersive characteristics shown by the instantaneous frequency structure corresponding to the first 6 modes of $\phi(t)$ in (1).

the mth mode is a time-shifted and dispersively frequency-shifted version of the transmitted waveform $x(t)$, i.e.,

$$y(t) = x(t-\tau)\mathrm{e}^{j2\pi f_m(t-\alpha^2)^{1/2}}\,. \qquad (2)$$

For shallow water environments characterized by dense multipath and continuous modal dispersions, we propose a representation of the received signal $y(t)$ as a weighted superposition of the basic signal transformation in (2), i.e.,

$$y(t) = \int_0^{T_d}\int_0^{F_m} H(\tau,\nu)x(t-\tau)\mathrm{e}^{j2\pi\nu(t^2-\alpha^2)^{\frac{1}{2}}}\,d\nu d\tau. \quad (3)$$

Specifically, we use the dispersive spreading function (DSF) $H(\nu,\tau)$ to quantify the transmitted energy associated with delay τ and cutoff frequency ν. In practice, since propagation loss increases with range and since higher modes suffer from more reflection loss, the DSF can be assumed to have a finite support $(\tau,\nu) \in [0,T_d]\times[0,F_m]$, where T_d is the multipath delay spread and F_m is the cutoff frequency for the highest mode of interest.

When the environment is randomly varying, the DSF $H(\tau,\nu)$ can be modeled as a stochastic process due to the uncertainty in the reflection spread in the (τ,ν)-plane. If the system responses at different time shifts and frequency dispersions are statistically uncorrelated, then the DSF can be completely characterized by its second-order statistics

$$\mathrm{E}[H(\tau,\nu)H^*(\tau',\nu')] = \Omega(\tau,\nu)\delta(\nu-\nu')\delta(\tau-\tau')\,, \quad (4)$$

where * denotes conjugation, $\mathrm{E}[\cdot]$ denotes expectation and $\delta(\cdot)$ is the Dirac delta function. The dispersive scattering function (DSC) $\Omega(\tau,\nu)$ provides a measure of the system power density in the (τ,ν)-plane.

3.2. Discrete Representation Model

The aforementioned model of the shallow water environment is based on a continuous formulation of the DSF. In practice, however, discrete frameworks are often more useful in increasing system performance. In this paper, we propose a mathematically equivalent discrete model to represent (3). Specifically, if the input signal $x(t)$ is bandlimited to $[-\frac{W}{2}, \frac{W}{2}]$, and the output signal $y(t)$ is defined for $t \in [t_0, t_1]$, $t_1 > t_0 > 0$, then we can decompose (3) into a weighted superposition of discrete time shifts and frequency dispersions to yield

$$y(t) \approx \sum_{l=0}^{L}\sum_{k=0}^{K} \hat{H}\left(\frac{l}{W}, \frac{k}{T}\right) x\left(t - \frac{l}{W}\right) \mathrm{e}^{j2\pi \frac{k}{T}(t^2-\alpha^2)^{\frac{1}{2}}} . \quad (5)$$

Here, $T = (t_1^2 - \alpha^2)^{1/2} - (t_0^2 - \alpha^2)^{1/2}$, and the summation limits are[1] $L = \lceil T_d W \rceil$ and $K = \lceil F_m T \rceil$. The samples $\hat{H}(\frac{l}{W}, \frac{k}{T})$ are obtained from the smoothed DSF given by

$$\hat{H}(\tau, \nu) = \int_0^{T_d}\int_0^{F_m} H(\tau', \nu') \mathrm{e}^{-j\pi\nu'\tau'} \mathrm{e}^{-j\pi(\nu-\nu')T} \cdot \mathrm{sinc}((\nu - \nu')T)\, \mathrm{sinc}((\tau - \tau')W) d\nu' d\tau' . \quad (6)$$

The discrete representation in (5) effectively samples the (τ, ν)-plane with a uniform grid. The sampling intervals are decided by the support of the dispersively transformed signal in time and frequency. Equation (5) effectively divides the received signal into $D = (K+1)(L+1)$ components, leading to a potential diversity system with diversity order upto D. Note that D is approximately proportional to the environment's spreading factor $F_m T_d$ and the time-bandwidth product TW of the transmitted waveform. The diversity implementation can be accomplished by a joint design of the transmitted waveform and RAKE receiver structure.

Next, we outline the major steps of sampling the time shift and dispersive frequency shift parameters to obtain (5) using two different approaches. The first approach is based on signal transformations whereas the second one depends on warping a unitarily equivalent narrowband system; both approaches yield the same discrete model.

3.2.1. Transform-based Approach

By defining $G(f, \nu)$ as the Fourier transform of $H(\tau, \nu)$ with respect to τ, we first rewrite (3) as

$$y(t) = \int_0^{F_m} \left[\int_{-\infty}^{\infty} G(f, \nu) X(f) \mathrm{e}^{j2\pi f t} df\right] \cdot \mathrm{e}^{j2\pi\nu(t^2-\alpha^2)^{\frac{1}{2}}} d\nu . \quad (7)$$

[1]Note that $\lfloor x \rfloor$ ($\lceil x \rceil$) rounds x to the integer nearest to zero (infinity).

Here, the Fourier transform $X(f)$ of $x(t)$ is assumed to be bandlimited to $[-\frac{W}{2}, \frac{W}{2}]$ and thus can be replaced by $X(f)\chi_{[-\frac{W}{2}, \frac{W}{2}]}(f)$, where $\chi_A(\cdot)$ is a unit amplitude rectangular window within the range of values defined by A. As a result, $\chi_{[-\frac{W}{2}, \frac{W}{2}]}(f) G(f, \nu)$ admits the following Fourier expansion,

$$\chi_{[-\frac{W}{2}, \frac{W}{2}]}(f) G(f, \nu) = \sum_l a_l(\nu) \mathrm{e}^{-j2\pi f \frac{l}{W}} \quad (8)$$

where the Fourier coefficient is given by

$$a_l(\nu) = \frac{1}{W}\int_{-\frac{W}{2}}^{\frac{W}{2}} G(f, \nu) \mathrm{e}^{j2\pi l \frac{f}{W}} df = \int_0^{T_d} H(\tau, \nu) \mathrm{e}^{-j\pi\nu\tau} \mathrm{sinc}\left(\left(\frac{l}{W} - \tau\right) W\right) d\tau , \quad (9)$$

and $\mathrm{sinc}(x) = \sin(\pi x)/(\pi x)$. Inserting (8) into (7), we obtain

$$y(t) = \int_0^{F_m} \sum_{l\in\mathbb{Z}} a_l(\nu) x(t - \frac{l}{W}) \mathrm{e}^{j2\pi\nu(t^2-\alpha^2)^{\frac{1}{2}}} d\nu = \sum_{l\in\mathbb{Z}} x(t - \frac{l}{W}) b_l((t^2 - \alpha^2)^{\frac{1}{2}}) \quad (10)$$

where we define

$$b_l(t) = \int_0^{F_m} a_l(\nu) \mathrm{e}^{j2\pi\nu t} d\nu . \quad (11)$$

As we have assumed that the output signal $y(t)$ is time-limited in $[t_0, t_1]$, both sides of (10) can be multiplied by $\chi_{[t_0,t_1]}(t)$. Applying the Fourier expansion to the resulting $b_l((t^2 - \alpha^2)^{\frac{1}{2}})\chi_{[t_0,t_1]}(t)$ and letting

$$\tilde{t}_0 = (t_0^2 - \alpha^2)^{\frac{1}{2}},\ \tilde{t}_1 = (t_1^2 - \alpha^2)^{\frac{1}{2}} , \quad (12)$$

leads to

$$b_l(t)\chi_{[\tilde{t}_0,\tilde{t}_1]}(t) = \sum_{k\in\mathbb{Z}} B_{l,k} \mathrm{e}^{j2\pi\frac{k}{T}t} , \quad (13)$$

where $T = \tilde{t}_1 - \tilde{t}_0$. The Fourier coefficient $B_{l,k} \equiv \hat{H}(\frac{l}{W}, \frac{k}{T})$; this follows since, using the definitions in (9) and (11),

$$\begin{aligned} B_{l,k} &= \frac{1}{T}\int_{\tilde{t}_0}^{\tilde{t}_1} b_l(t) \mathrm{e}^{-j2\pi k\frac{t}{T}} dt \\ &= \frac{1}{T}\int_{\tilde{t}_0}^{\tilde{t}_1}\int_0^{F_m} a_l(\nu) \mathrm{e}^{j2\pi\nu t} d\nu\, \mathrm{e}^{-j2\pi k\frac{t}{T}} dt \\ &= \int_0^{F_m} a_l(\nu) \mathrm{e}^{j\pi(\nu-\frac{k}{T})(\tilde{t}_0+\tilde{t}_1)} \mathrm{sinc}\left(\left(\frac{k}{T} - \nu\right) T\right) d\tau d\nu \\ &\approx \int_0^{T_d}\int_0^{F_m} H(\tau, \nu) \mathrm{e}^{-j\pi(\frac{k}{T}-\nu)T} \\ &\cdot \mathrm{sinc}\left(\left(\frac{k}{T} - \nu\right) T\right) \mathrm{sinc}\left(\left(\frac{l}{W} - \tau\right) W\right) d\tau d\nu . \quad (14) \end{aligned}$$

The last approximation follows from $(\tilde{t}_0 + \tilde{t}_1) \approx T$ when $t \gg \alpha$. Also note that if $H(\tau,\nu)$ has a finite support $(\tau,\nu) \in [0,T_d] \times [0,F_m]$, then the weighting coefficients in (14) are significantly nonzero only if the mainlobe of the smoothing functions $[(l-1)/W,(l+1)/W]$ and $[(k-1)/T,(k+1)/T]$ are effectively overlapped with the time-shift support $[0,T_d]$, and the frequency-shift support $[0,F_m]$, respectively. Thus, choosing $0 \le l \le \lceil T_d W \rceil$ and $0 \le k \le \lceil F_m T \rceil$, replacing (14) into (13) and then into (10), finally yields (5).

3.2.2. *Warping-Based Approach*

A narrowband system $\mathcal{L}$ can be represented as a weighted superposition of time-frequency shifted versions of the input signal $x(t)$:

$$(\mathcal{L}x)(t) = \int_{-\infty}^{\infty}\int_{-\infty}^{\infty} \mathrm{SF}_{\mathcal{L}}(\tau,\nu)(\mathcal{M}_\nu \mathcal{S}_\tau x)(t)\, d\nu\, d\tau\,. \quad (15)$$

The frequency shift operation and time shift operation on the signal are defined, respectively, by $(\mathcal{M}_\nu x)(t) = x(t)\,\mathrm{e}^{j2\pi\nu t}$ and $(\mathcal{S}_\tau x)(t) = x(t-\tau)$. If we assume that the input signal $x(t)$ is bandlimited to $[f_0, f_1]$ with bandwidth $W = f_1 - f_0$, and that the output signal $(\mathcal{L}x)(t)$ is time-limited to $[t_0,t_1]$ with duration $T = t_1 - t_0$, then (15) can be decomposed into [9]

$$(\mathcal{L}x)(t) = \sum_{l\in\mathbb{Z}}\sum_{k\in\mathbb{Z}} \widehat{\mathrm{SF}}_{\mathcal{L}}(\frac{l}{W},\frac{k}{T})\,(\mathcal{M}_{\frac{k}{T}}\mathcal{S}_{\frac{l}{W}}x)(t) \qquad (16)$$

where $\widehat{\mathrm{SF}}_{\mathcal{L}}(\frac{l}{W},\frac{k}{T})$ are two-dimensional samples of the smoothed SF

$$\widehat{\mathrm{SF}}_{\mathcal{L}}(\tau,\nu) = \int_{-\infty}^{\infty}\int_{-\infty}^{\infty} \mathrm{SF}_{\mathcal{L}}(\tilde{\tau},\tilde{\nu})\mathrm{e}^{-j\pi(\nu-\tilde{\nu})(t_0+t_1)}\,\cdot$$
$$\mathrm{e}^{j\pi(\tau-\tilde{\tau})(f_0+f_1)}\mathrm{sinc}((\nu-\tilde{\nu})T)\mathrm{sinc}((\tau-\tilde{\tau})W)d\tilde{\nu}d\tilde{\tau} \quad (17)$$

sampled at the uniform grid $\tau = \frac{l}{W}$ and $\nu = \frac{k}{T}$.

Figure 2 demonstrates the unitary warping relation between the narrowband system $\mathcal{L}$ and the dispersive shallow water system that we denote here by $\mathcal{D}$. The input and output of the dispersive system are $x(t)$ and $(\mathcal{D}x)(t)$ (which corresponds to $y(t)$ in (3)), respectively. The unitary warping transformation $\mathcal{U}$ is defined as

$$(\mathcal{U}x)(t) = \frac{t^{1/2}}{(t^2+\alpha^2)^{1/4}} x((t^2+\alpha^2)^{1/2}) \qquad (18)$$

and inverse warping is such that $(\mathcal{U}^{-1}\mathcal{U}x)(t) = x(t)$. Specifically, the unitary warping relation converts a dispersive system into a narrowband system. This follows as the unitarily equivalent system $\mathcal{L} = \mathcal{U}\mathcal{D}\mathcal{U}^{-1}$ is narrowband [10] if the DSF $H(\tau,\nu)$ of the dispersive system $\mathcal{D}$ is related to the SF of the warped system $\mathcal{L}$ as

$$H(\tau,\nu) = \mathrm{SF}_{\mathcal{U}^{-1}\mathcal{D}\mathcal{U}}(\tau,\nu)\,. \qquad (19)$$

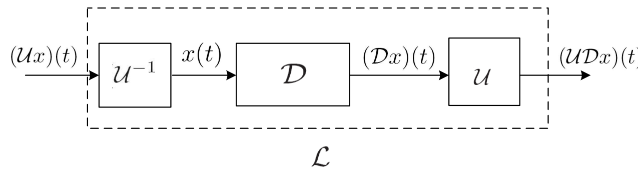

Fig. 2. The warping relation between the shallow water dispersive system $\mathcal{D}$ and the unitarily equivalent narrowband system $\mathcal{L} = \mathcal{U}\mathcal{D}\mathcal{U}^{-1}$.

Since we have assumed that $x(t)$ is bandlimited to $[-\frac{W}{2},\frac{W}{2}]$, the input signal $(\mathcal{U}x)(t)$ of the composite system is also approximately bandlimited to $[-\frac{W}{2},\frac{W}{2}]$; this follows from (18) when $t \gg \alpha$ and thus it is reasonable to approximate $(\mathcal{U}x)(t) \approx x(t)$. On the other hand, since we have assumed that the output signal $(\mathcal{D}x)(t)$ of the dispersive system is time-limited to $[t_0,t_1]$, we conclude from (18) that the warped signal $(\mathcal{U}\mathcal{D}x)(t)$ is time-limited to $[\tilde{t}_0,\tilde{t}_1]$ where $\tilde{t}_0$ and $\tilde{t}_1$ are defined in (12).

Based on the above assumptions on the signals time-frequency supports, and using the narrowband discrete formulation in (16), the equivalent narrowband system $\mathcal{U}\mathcal{D}\mathcal{U}^{-1}$ can be discretized as,

$$(\mathcal{U}\mathcal{D}x)(t) = \sum_{l\in\mathbb{Z}}\sum_{k\in\mathbb{Z}} \widehat{\mathrm{SF}}_{\mathcal{U}\mathcal{D}\mathcal{U}^{-1}}(\frac{l}{W},\frac{k}{T})(\mathcal{M}_{\frac{k}{T}}\mathcal{S}_{\frac{l}{W}}\mathcal{U}x)(t) \quad (20)$$

where $T = \tilde{t}_1 - \tilde{t}_0$ and the smoothed SF $\widehat{\mathrm{SF}}_{\mathcal{U}\mathcal{D}\mathcal{U}^{-1}}(\tau,\nu)$ can be determined by (17). Note that because of the warping relation (19), $\widehat{\mathrm{SF}}_{\mathcal{U}\mathcal{D}\mathcal{U}^{-1}}(\frac{l}{W},\frac{k}{T}) \equiv \hat{H}(\frac{l}{W},\frac{k}{T})$, where $\hat{H}(\tau,\nu)$ is the smoothed DSF in (6). Thus, applying $\mathcal{U}^{-1}$ to both sides of (20), based on the fact that $\mathcal{U}_\xi^{-1}$ is a linear transformation, we can obtain the discretization in (5). This follows since, using (18), we obtain the dispersive frequency shift as

$$(\mathcal{U}^{-1}\mathcal{M}_{\frac{k}{T}}\mathcal{U}x)(t) = \mathrm{e}^{j2\pi\frac{k}{T}(t^2-\alpha^2)^{\frac{1}{2}}}x(t)\,,$$

and, when $t \gg \alpha$, the approximated time shift as

$$(\mathcal{U}^{-1}\mathcal{S}_{\frac{l}{W}}\mathcal{U}x)(t) \approx x\left(t - \frac{l}{W}\right)\,.$$

4. WAVEFORM DESIGN FOR DIVERSITY

As we described in the previous section, the dispersive environment of shallow water can be represented by (3) and (5). In this section, we propose to design an appropriate waveform to exploit the dispersion characteristic of the environment together with its discrete model in (5) to provide diversity in shallow water communications.

We consider the case where the environment does not introduce multipath but only dispersive Doppler shifts.

This assumption is reasonable when a strong path plays a dominant role over all other paths from the transmitter to the receiver. This path has time delay l_0/W and different dispersive Doppler components k/T for $k = 0, \ldots, K$. Without loss of generality, we can assume that $l_0 = 0$, and the discrete dispersive environment model in (5) simplifies to

$$y(t) = \sum_{k=0}^{K} h_k x(t) e^{j2\pi \frac{k}{T}(t^2-\alpha^2)^{1/2}} \tag{21}$$

where $h_k = \hat{H}(0, \frac{k}{T})$. The actual received signal can be represented as

$$r(t) = y(t) + n(t)$$

where $n(t)$ is additive white Gaussian noise (AWGN). We also consider binary antipodal modulation in (21) as

$$x(t) = b\, s(t) \tag{22}$$

where $b = \pm 1$ is the transmitted information bit and $s(t)$ is the modulation waveform function.

At the receiver, we can use a RAKE receiver to estimate the transmitted information bit as

$$\hat{b} = \text{sign}\left(\text{Re}\left\{ \sum_{k=0}^{K} h_k^* \int_{t_0}^{t_1} r(t) s_k^*(t) dt \right\} \right) \tag{23}$$

where Re$\{\cdot\}$ denotes the real part. Here, the kth dispersively frequency-shifted version of $s(t)$ is given by $s_k(t) = e^{j2\pi \frac{k}{T}(t^2-\alpha^2)^{\frac{1}{2}}} s(t)$.

In order to exploit the potential dispersive Doppler diversity of the environment, we need to design the waveform $s(t)$ of the transmitted signal to match the shallow water environment characteristics, so that the RAKE receiver in (23) can perform MRC. To exploit the dispersive Doppler diversity, the transmitted signal $x(t)$ must also satisfy the following orthogonality condition:

$$\int_{t_0}^{t_1} x_k(t) x_{k'}^*(t) dt = C\, \delta[k - k'] \tag{24}$$

where $C > 0$ is a constant, $\delta[\cdot]$ is the Kronecker delta function and

$$x_k(t) = x(t) e^{j2\pi \frac{k}{T}(t^2-\alpha^2)^{1/2}}, \quad \text{for } t \in [t_0, t_1]\,. \tag{25}$$

In order to satisfy the orthogonality condition in (24), we design a wideband waveform function

$$s(t) = \frac{t^{1/2}}{(t^2-\alpha^2)^{1/4}} e^{j2\pi\beta(t^2-\alpha^2)^{1/2}}\,. \tag{26}$$

Note that $s(t)$ is a time-varying signal with frequency-modulation rate β, and its instantaneous frequency can be represented as

$$\frac{d}{dt}\beta(t^2-\alpha^2)^{1/2} = \beta t/(t^2-\alpha^2)^{1/2}\,.$$

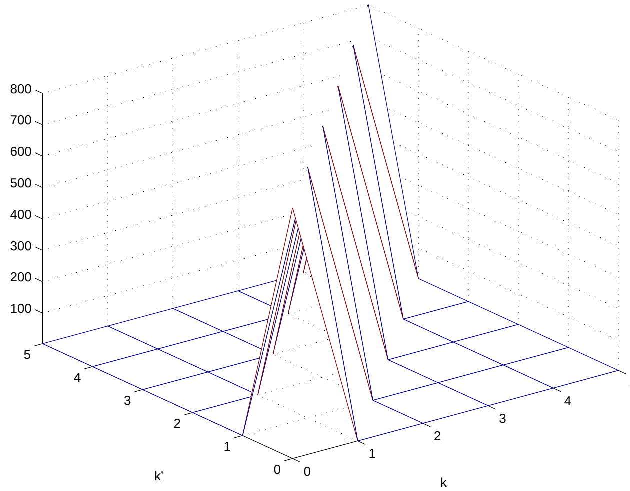

Fig. 3. Numerically computed correlation values of Equation (27) to demonstrate the validity of the orthogonality condition.

By designing the waveform according to (26), we ensure that the instantaneous frequency of $s(t)$ matches the time-frequency structure of the dispersive characteristics of the shallow water environment as shown in Figure 1.

To verify the orthogonality condition, we substitute (26) into (22) and then $x(t)$ into (25). The resulting expression is then substituted into (24) to obtain

$$\begin{aligned}\int_{t_0}^{t_1} x_k(t) x_{k'}^*(t) dt &= T e^{j\pi \frac{k-k'}{T}(\tilde{t}_1+\tilde{t}_0)} \text{sinc}\,(k-k') \\ &= T\delta[k-k']\end{aligned} \tag{27}$$

and the orthogonality condition (24) is satisfied. This is further demonstrated by the plot of the numerically evaluated correlation values for varying k and k' in (27) using $\alpha = 20$, $t_0 = 200$, $t_1 = 1000$ and $K = 5$ in Figure 3. Thus, at the receiver, we can resolve the transmitted signal from these $K+1$ dispersive Doppler components and gain a $(K+1)$th order diversity using MRC assuming the environment parameters h_k in (21) are known.

5. PERFORMANCE ANALYSIS

To demonstrate the advantage of choosing the matched waveform to obtain the desired diversity gain from the dispersive shallow water environment, we consider a performance analysis and numerical results in this section. Specifically, we compare our proposed wideband waveform in (26) with the narrowband sinusoidal waveform.

For notational convenience, we concatenate the aforementioned waveforms (or coefficients) based on their frequency index k, into the following $(K+1)$-dimensional vectors:

$$\begin{aligned} \mathbf{h} &= [h_0 \ldots h_k \ldots h_K]^\top \\ \mathbf{s}(t) &= [s_0(t) \ldots s_k(t) \ldots s_K(t)]^\top \\ \mathbf{x}(t) &= [x_0(t) \ldots x_k(t) \ldots x_K(t)]^\top \end{aligned}$$

where $\top$ denotes transpose.

For binary signals using the RAKE receiver in (23), the bit error rate (BER) is given by [11]

$$P_b = \frac{1}{\pi} \int_0^{\pi/2} \prod_{k=0}^{K} \left(1 + \frac{\gamma_b \lambda_k}{\sin \theta^2}\right)^{-1} d\theta \,. \tag{28}$$

Here, γ_b is the average signal-to-noise ratio (SNR) per bit, and λ_k are the eigenvalues of the matrix

$$\mathbf{\Sigma} = \mathbf{R_{xs}} \mathbf{\Omega_h} \mathbf{R_{xs}}^\dagger \tag{29}$$

where $\dagger$ denotes Hermitian operation. $\mathbf{R_{xz}} = \int_t \mathbf{x}(t)\mathbf{s}^\dagger(t)dt$ is the cross-correlation matrix of the waveform vectors $\mathbf{x}(t)$ and $\mathbf{s}(t)$, and $\mathbf{\Omega_h} = \mathrm{E}[\mathbf{hh}^\dagger]$ is the correlation matrix of the coefficient vector $\mathbf{h}$ that can be evaluated using (6) and the uncorrelated assumption in (4). Specifically, its (k,k')th, $k,k' = 0,\ldots,K$, element is given by

$$\mathrm{E}[h_k h^*_{k'}] = \int_0^{F_m} H(\frac{l_0}{W}, \nu) \mathrm{sinc}\,(k' - \nu T)\,\mathrm{sinc}\,(k - \nu T)\, d\nu \,. \tag{30}$$

From (28), the effective diversity order is the rank of $\mathbf{\Sigma}$ in (29). In the special case of an orthonormal $\mathbf{R_{zx}}$, $\mathbf{\Sigma}$ has the same rank as that of the system correlation matrix $\mathbf{\Omega_h}$. Furthermore, from (30), if the DSC $\Omega(\tau,\nu)$ has a sufficiently smooth shape, and if, after the time-frequency sampling and smoothing, all K diversity components have significantly nonzero energy and are correlated at most partially, then the correlation matrix $\mathbf{\Omega_h}$ will have full rank K. If these constraints for the environment and the transceiver implementation are satisfied, the diversity system can achieve the full diversity order of K.

Figure 4 illustrates the numerical result of the BER performance for two different waveforms for the dispersive shallow water communication environment. Here, the symbol duration is $T = 20$ ms, $L = 0$, and $F_m = 50, 100$, and 150 Hz resulting in $K = 1, 2$, and 3, respectively. The solid lines represent our proposed waveform in (26) that is matched to the system's dispersive characteristics. The dashed lines represent sinusoidal waveforms (that is, $s(t) = 1$ in the baseband representation). It can be clearly seen from the figure that our proposed matched waveform outperforms non-matched waveforms in that the former can exploit the potential diversity from our proposed dispersive shallow water environment model.

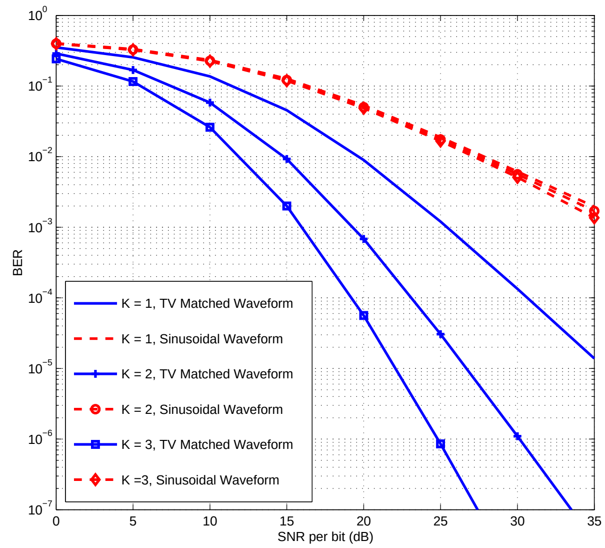

Fig. 4. BER performance comparison of different waveforms. Solid lines: time-varying (TV) waveform matched to the environment, dashed lines: sinusoidal waveform.

6. CONCLUSION

In this paper, we developed a time-varying system representation to describe the dispersive propagation characteristics of shallow water acoustic environments. Furthermore, through a transform-based approach as well as a warping-based approach, we developed the discrete model of the time-varying dispersive representation. Using this discrete model in a shallow water communication application, we designed a wideband time-varying waveform for the transmitted signal to match the dispersive nature of the environment. As we demonstrated with performance analysis and numerical results, by employing the maximal ratio combining technique, our designed waveform can exploit dispersive Doppler diversity.

Acknowledgments

This work was supported in part by the NSF CAREER Award CCR-0134002 and the Department of Defense Grant No. AFOSR FA9550-05-1-0443.

7. REFERENCES

[1] L. J. Ziomek, *Underwater Acoustics: A Linear Systems Theory Approach*, Academic Press, Orlando, FL, 1985.

[2] P. A. Bello, "Characterization of randomly time-variant linear channels," *IEEE Transactions on Communications*, vol. 11, May 1963.

[3] A. M. Sayeed and B. Aazhang, "Joint multipath-Doppler diversity in mobile wireless communications," *IEEE Transactions on Communications*, vol. 47, pp. 123–132, January 1999.

[4] J. G. Proakis, *Digital Communications*, McGraw-Hall, Inc., 4 edition, 2001.

[5] I. Tolstoy and C. S. Clay, *Ocean Acoustics: Theory and Experiment in Underwater Sound*, McGraw-Hill Book Company, 1966.

[6] J.-P. Hermand and W. I. Roderick, "Acoustic model-based matched filter processing for fading time-dispersive ocean channels: Theory and experiment (invited paper)," *IEEE Journal on Oceanic Engineering*, vol. 18, pp. 447–465, October 1993.

[7] M. Stojanovic, "Recent advances in high-speed underwater acoustic communications," *IEEE Journal on Oceanic Engineering*, vol. 21, pp. 125–136, April 1996.

[8] C. Chen, H. M. James, G. F. Boudreaux-Bartels, R. P. Gopu, and J. L. Colin, "Time-frequency representations for wideband acoustic signals in shallow water," in *OCEANS*, September 2003, vol. 5, pp. 2903–2907.

[9] Y. Jiang, *Discrete Characterizations of Wideband and Dispersive Time-Varying Systems*, Ph.D. thesis, Arizona State University, Tempe, AZ, Nov. 2005.

[10] B. G. Iem, A. Papandreou-Suppappola, and G. F. Boudreaux-Bartels, "Wideband Weyl symbols for dispersive time-varying processing of systems and random signals," *IEEE Transactions on Signal Processing*, vol. 50, pp. 1077–1090, May 2002.

[11] Y. Jiang and A. Papandreou-Suppappola, "Discrete time-frequency characterizations of dispersive time-varying systems," *IEEE Transactions on Signal Processing*, 2005, (submitted).